Updating finite element model of façade scaffolds anchor considering experimental data

Jakub Dolejš

Faculty of Civil Engineering – Department of Steel and Timber Structures, Czech Technical University in Prague, Thakurova 7, 166 29 Praha 6, Czech Republic

Vikas Arora

Department of Technology and Innovation, University of Southern Denmark, Campusvej 55, Odense 5230, Denmark

Jiri Ilcik,
J2L CONSULT, s.r.o., Brandlova 2536/36, 69501, Hodonin, Czech Republic

ABSTRACT

Considering the stability of the façade scaffolds, the anchoring is one of the most important phenomenon. The anchors secure scaffolding against the overturning also transferring the horizontal forces from the scaffold into the façade. There are many different types of the anchors in a construction field, but the same principle is used to join these anchors to the thermal insulated façade. A new type of façade scaffold anchor was developed and described in this paper. Main problems associated with the existing anchors are: damage of façade thermal insulation layers, insufficient supporting of the scaffold standards and decreasing the stability of the scaffold construction. The new developed anchor overcomes the problems associated with the existing anchoring. The experiment of the developed anchor has been carried out and it has been observed that the experimental results (force–displacement curve) do not match with the finite element predictions. Subsequently the finite element model (FEM) of the developed anchor has been updated in the light of experimental results. The finite element model of the anchor is corrected using the parameter-based finite element model updating method. The results have shown that there is a good correlation between the updated finite element model and the experimental data. The accuracy of updated finite element model is demonstrated by plotting the predictions made by finite element model with experimental results. The overlay of finite element model predictions and experimental data has shown the success of the updating procedure and thus it can accordingly be concluded that updated finite element model of the anchor represents the reality with confidence.

Keywords: Parameter-based optimization; Stability-based anchor design; Experimentation of anchor, Finite element model of anchor, Façade scaffolds.

INTRODUCTION

A use of façade thermal insulation layers for new buildings as well as for the existing constructions is a quite common phenomenon. But none of existing fixing methods of the scaffold structures considers these layers. For the best anchoring, a scaffold's tie member is pinned as nearest to a façade as possible (Dolejš, 2013). In this way, the insulation layer has to be removed, which requires additional repairs. Other more common option is to use a long scaffold screw, which connects tie member and façade as it is shown in Figure 1. Because of the safety, nowadays, scaffolds systems are covered with nets or planks. However, the cladding increases horizontal force acting on anchors (Vlasák, 2011), under the impact of the wind load, which is crucial in the most of the accident cases (Wang *et al.*, 2013; Wang *et al.*, 2014) the long scaffold screw can hardly transmit the forces from the scaffold construction into the façade, which results in a deformation of the screw as well as damage of the surrounding thermal layers and the stiffness of the whole scaffold system is considerably decreased (Dolejš, 2013). It should also be noted that due to loosed connections of components (Chandrangsu and Rasmussen, 2009), the scaffold system becomes weak which brings difficulties in stabilizing the construction and anchoring (Beale, 2014). The stability of the frame scaffoldings has been observed in many papers, see (Liu *et al.*, 2010; Peng *et al.*, 2013). The insufficient stability of the tube scaffoldings is described by Dolejs, 2013. The scaffolding has been modeled according to the netted cladding and the values and load combinations have been based

on European standards EN 12 811-1 (2003). The anchors have been modeled as a pinned supports. The scaffold´s tubes have been connected by semi-rigid joints respecting M – φ relation obtained by the experiment. Generally the semi-rigid connections as well as initial imperfections have a significant impact on the results (Prabhakaran *et al.*, 2011; Chandrangsu and Rasmussen, 2011). Critical load coefficients for each combination were computed. The values vary in the range from 1.68 to 2.74 only. If the same model is supported by a rigid fixing, then the critical coefficient values became higher even if the number of the anchors decreased.

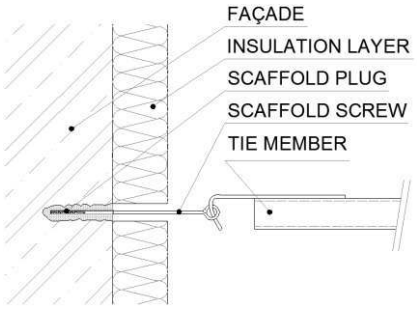

Figure 1 - Vertical section of the plugged anchor – because of an insulation layer a long screw is used

Based on these analyses, it was determined that a potential newly developed anchor should provide a rigid-torsion support in a horizontal plane. It is obvious that final behavior of a real anchor will be semi-rigid, but however even a semi-rigid support could have a large impact on the complex stability (Peng *et al.,* 2009; Beale and Godley, 2009)
For further analyses and a development the tubular scaffold systems has been mainly considered. The reasons are that a tubular scaffold is generally a weaker system then a frame scaffold (Dolejš *et al.*, 2011; Chandrangsu and Rasmussen, 2011) and because of that the support forces in tubular scaffolding are greater.

PROPOSED ANCHOR DESIGN

In order to overcome the problems associated with the existing anchoring three shapes of the new anchor have been developed and officially registered. The original design of these anchors has been made by the simple empiric way. Three models has been termed as type I (The Rigid Scaffold Anchor), type II (The Oblique Scaffold Anchor) and type III (The Oblique Sliding Scaffold Anchor). For the following study, the type III has been used. Type III is represented by a main part which is an oblique and adjustable arm. It can be observed from Figure 2, that at least two anchors in one horizontal plane must be used in a fixing system, these two anchors placed in the opposite orientation have to create a notional trapezoid with the surface of the façade. If the outer plane seems to be stiff enough because of the vertical X-bracing, the inner plane can be moved only in way parallel with the façade. By using the type III anchors the displacement of the inner plane should be also restricted. Next advantage is that this anchor enables only a minimum displacement of the parallel threaded rods which are jointed into the façade and that ensures the non-damaging of the surrounding insulation layers.

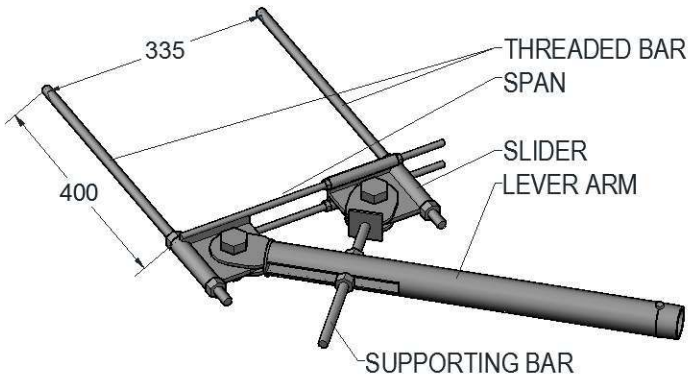

Figure 2 - Type III Anchor

Details of particular parts are presented in Figure 4, brief description follows. The main part consists of two threaded bars with a circular cross section M16 /8.8. Bars are plugged into the façade while the thermal insulation layers are surrounding these two bars. The members “Span” and “Slider” are put on “Threaded bars”. “Slider” is made of steel plates with thickness 7 mm and of the steel tubes with dimension 48.3/3.2 class of steel S235J0. The “Slider” is also providing a base for the “Supporting bar”. The “Span” member is basically of the same shape as the “Slider”, but there are two parallel threaded rods M10 /4.8. welded on it. Because of the rods´ length, the “Threaded bars” could be in any mutual distance up to 400 mm. Furthermore, the distance between the “Span” and the façade depends on a depth of insulation layers. The “Threaded bars”, “Slider” and “Span” create a rigid frame. The “Supporting bar” fixes the position of the “Lever arm”. The cross section of the bar is M16 /8.8. The “Lever arm” is made of the classic scaffold tube with dimensions 48.3/3.2 mm class of steel S235J0. The end of the “Lever arm” is connected with the scaffold´s standard. For the connections of the members to each other there are two bolts M16 /8.8. Used parts connected by this way are naturally hinged with free rotations.

EXPERIMENT

The scheme diagram of the laboratory experiment is shown in Figure 3. The anchor was plugged into the fixed steel beam and loaded continually by tension force only in vertical direction. The force rose from 0 up to 3 kN and the dependence of a displacement of the lever arm was recorded in real time. Output of the experiment was a force-displacement curve (Figure 4).

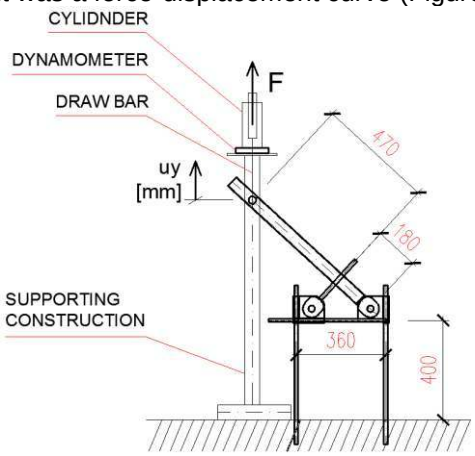

Figure 3 - The vertical section of the laboratory experiment

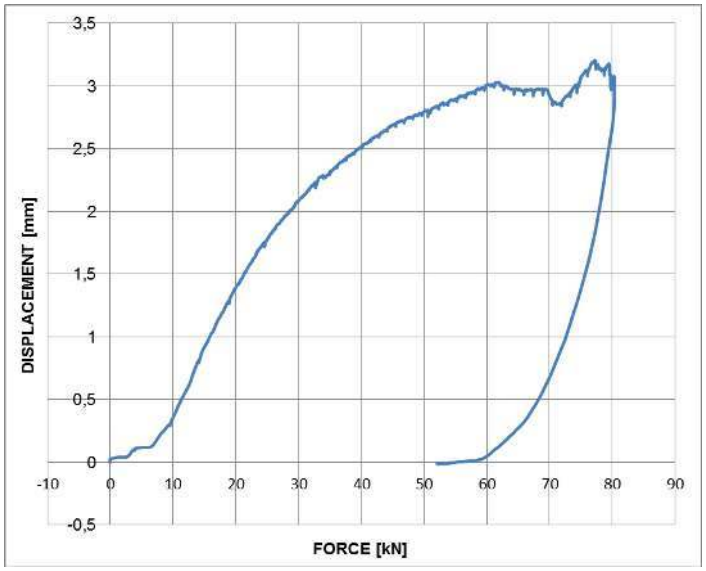

Figure 4 - The final Force – Displacement curve of the experiment

The force was provided by the single acting hollow plunger cylinder ENERPAC RCH-123 with the one-handed pump ENERPAC P-392 (Enerpac data sheet, 2010). The cylinder was situated on the

top of the supporting steel construction made from two parallel columns with reversed T shape. This construction was surrounding the Lever arm of the anchor. Between the cylinder and the upper surface of the construction was placed a tensometric pressure dynamometer S35 (Tensiometric dynamometer S-35 data sheet, 2011), which was connected with the computer to measure an actual loading force. The draw bar made of steel was connecting a hydraulic cylinder to the end of Lever arm. The output of this experiment was a vertical displacement of the lever arm. This displacement was measured by the common absolute potentiometer sensor and real-time values were transferred into the computer. It seems that at a very beginning the "Span bar" reached the plastic behavior. After applying the force of approximately 3.0 kN the first small cracks on the span´s bars have been detected, these cracks become larger at the end of the experiment. The weakest part of the anchor seems to be the Span member.

THE ANCHOR ANALYSIS

For numerical analysis both beam and solid model have been developed. In these models the applied force rose from 0 up to 3.0 kN and the maximum deflection (u_y) at the end of the Lever arm should be 60 mm (according to the Figure 4). As it is observed from the experiment the anchor is deformed permanently, materially non-linear beam and solid models of anchor are developed.
In the FE models, the cross sections of the all threaded rods are considered with the value of minor diameter. Also it has to be mentioned that the real anchor consists of several single parts with the gaping between each other. Because of that the initial displacement ($u_{y,initial}$) of the measured Lever arm was set up as 10 mm.

The Initial beam model

The beam model was created in ANSYS workbench. Geometry of the FE model corresponds to the geometry of the experimental anchor. The model consists of 9 parts with 455 nodes and 226 elements, total weight is 4,91 kg (Figure 5). Parts 03 and 04 are not expected to be deformed, so they are simply modeled as rigidly connected beams with a circular cross section with the diameter 13.0 mm. The member Lever arm consists of two parts, because of the different cross sections. The longer main part of Lever arm has a cross section of steel scaffold tube. The shorter part, which is closer to the Span bar, should have a cross section of weakened scaffold tube, but since there was no occurring deformation during the experiment this part has been simply modeled as the scaffold tube too. Cross sections of other members were introduced in the text above.

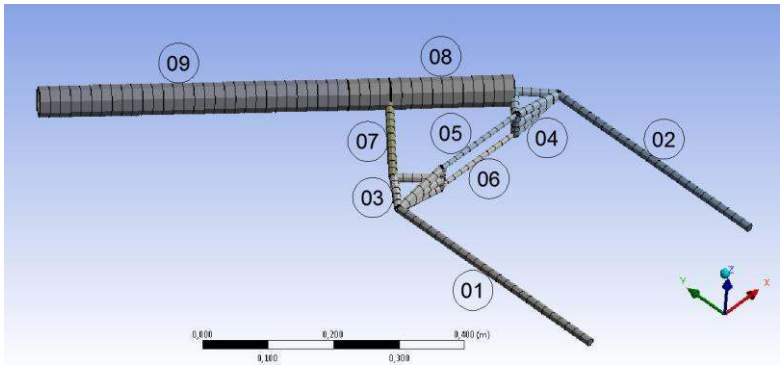

Figure 5 - The beam model, Parts: 01-Left Threaded Bar, 02-Right Threaded Bar, 03-Slider, 04-Span Bar (base), 05-Span Bar (Upper rod), 06-Span Bar (Bottom rod), 07-Support Rod. 08 and 09-Lever Arm

Also values of the yield strengths of the materials were initially estimated. The three non-linear materials are used for the models. The structural steel S235 has 200 MPa of the yield strength, steel classes used for rods 4.8 and 8.8 have 300 and 580 MPa. Plastic behavior of these materials has been expected, so the working diagrams are considered as bilinear with isotropic hardening. Young modulus of all materials is 210 GPa.
Single members of the anchor were connected together with a both of the longitudinal (along X and Y axes) and also with torsional stiffness (along the Z axis). Table 1 summarizes degrees of freedom of each joint, the bolted joints (3-7 and 4-8 according to Table 1) are considered as hinged connections. The initial values of longitudinal stiffness were computed using empiric equations. But

the real values of these joint stiffnesses are unknown and they are considered to be the source of error in the finite element model.

Table 1 - Degrees of freedom in joints

PARTS	JOINT NAME	X	Y	Z	ROT X	ROT Y	ROT Z
		[MN/m]			[MNm/rad]		
1 - 3	L	1470	406,9	free	free	free	0,1
2 - 4	R	1470	406,9	free	free	free	0,1
3 - 5	LN-U	351,9	9000	free	free	free	0,01
3 - 6	LN-D	351,9	9000	free	free	free	0,01
4 - 5	RN-U	387,9	21630	free	free	free	0,1
4 - 6	RN-D	387,9	21630	free	free	free	0,1
3 - 7	/	rigid	rigid	rigid	free	free	free
4 - 8	/	rigid	rigid	rigid	free	free	free
7 - 8	/	rigid	rigid	rigid	free	free	free
8 - 9	/	rigid	rigid	rigid	rigid	rigid	rigid

The defection profile is calculated using the applied force and subsequently plotted along with the experimental results and it can be observed from the Figure 6 that the finite element results do not match with the experimental results.

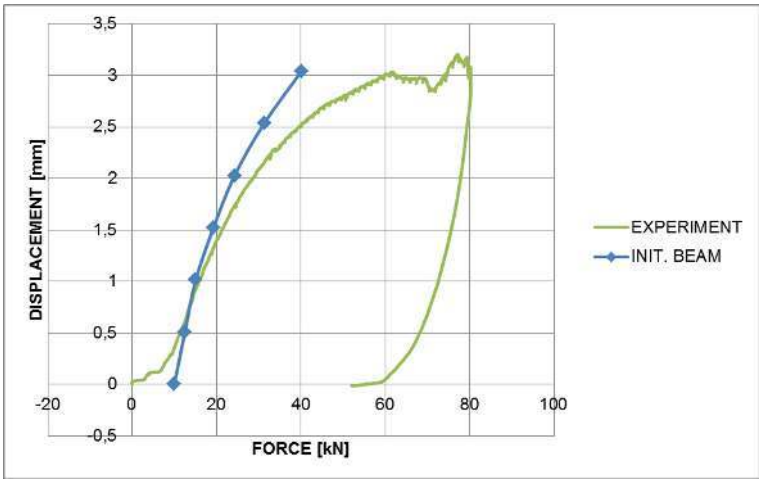

Figure 6 - Force – Displacement curve of the Initial beam model

The Initial solid model

The solid model has been also created in ANSYS workbench, as shown in Figure 7, indications of the parts can be also given in this figure. The model consists of 11 parts. The mesh contains 30 415 nodes and 16 457 elements. As it was expected and according to the higher accuracy the total weight 7.57 kg is significantly more than the beam model weight (4.91 kg). All connections between FE were set up as joints. Cross sections and material properties have been used the same like for the beam model. Since the connections were entered as joints, in solid model the optimization parameters will be material properties only.

The output force-displacement curve is represented in the Figure 8 and as it was expected the curve also do not match with the experimental data perfectly.

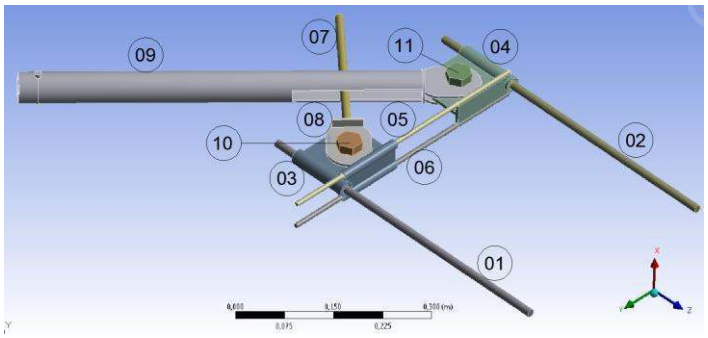

Figure 7 - The solid model, 01-Left Threaded Bar, 02-Right Threaded Bar, 03-Slider, 04-Span Bar (base), 05-Span Bar (Upper rod), 06-Span Bar (Bottom rod), 07-Support Rod, 08-Support Rod (base), 09-Lever Arm, 10-Left Bolt, 11-Right Bolt

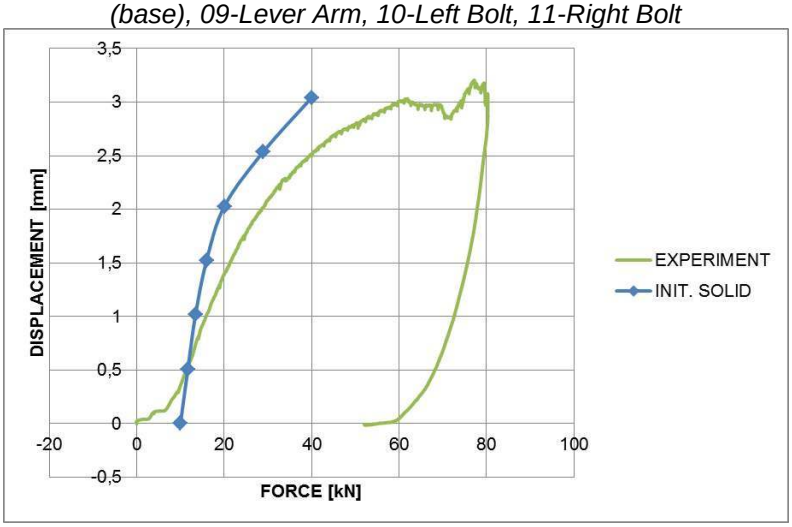

Figure 8 - Force – Displacement curve of the initial solid model

OPTIMIZATION

Choice of updating parameters on the basis of engineering judgment about the possible locations of modelling errors in a structure is one of the strategies to ensure that only physical meaningful corrections are made. In case of an anchor, modelling of stiffness of the joints and the values of the material is expected to be a dominant source of inaccuracy in the FE model, assuming that and the geometric parameters are correctly known. The values of stiffness of joints and values of the material parameters are updated in the light of experimental results. Some work has been carried out to update the stiffness of joint in the light of experimental data. Arora et al. (2009) updated the joint stiffness of a F-shape structure using frequency response function data. The joints include both bolted and welded joints. Arora (2014) updated stiffness of the end of cantilever beam using resonance and anti-resonance frequencies. Gant et al. (2011) updated joint stiffness of large aeronautical structures. Okasha et al. (2012) updated the finite element models of bridges using strain data for lifetime reliability assessment of the bridges. All the above mentioned methods of updating the finite element models are sensitivity based methods in which the sensitivities of parameters are used to reduce the error between the finite element predictions and experimental data.

Parameter-based finite element model updating using defection

Updating method is an iterative and parameter-based model updating method and uses defections to update the finite element model. Following identities relating to stiffness (K) and deflection (Q) relating to analytical model as well as actual structure respectively can be written as:

$$k_A Q_A = F \quad (1)$$

$$k_X Q_X = F, \quad (2)$$

where subscript A and X denotes an analytical (FE model) and experimental model respectively. As right hand side of Eqs. 1 and 2 is same. It can written as:

$$k_A Q_A = k_X Q_X \quad (3)$$

Considering experimental stiffness value is greater than analytical stiffness value. Experimental stiffness value can be written as:

$$k_X = k_A + \Delta k \quad (4)$$

Substituting Eq. 4 in Eq. 3 as:

$$k_A Q_A = (k_A + \Delta k) Q_X \quad (5)$$
$$k_A Q_A - k_A Q_X - \Delta k\, Q_X = 0 \quad (6)$$
$$k_A (Q_A - Q_X) - \Delta k\, Q_X = 0 \quad (7)$$
$$\frac{\Delta k\, Q_X}{k_A} = Q_A - Q_X \quad (8)$$
$$\Delta k = k_A \frac{Q_A - Q_X}{Q_X} \quad (9)$$

Eq. (9) is the basic equation of updating the stiffness matrix using defection. Analytical stiffness of structure consists of individual element stiffness as:

$$k_A = \sum_{i=1}^{n} k_i, \quad (10)$$

where *n* is number of elements. Linearizing Δk with respect to the {*p*}, {*p*}={$p_1, p_2, \ldots, p_{nu}$}, where *nu* is number of updating parameters, being the vector of updating variables associated with individual or group of finite elements, gives:

$$\Delta k = \sum_{j=1}^{nu} \left(\frac{\partial k_j}{\partial p_j} \Delta p_j \right) \quad (11)$$

Dividing and multiplying above equation by p_j and then writing u_j in place of $\Delta p_j / p_j$, the equation becomes:

$$\Delta k = \sum_{j=1}^{nu} \left(\frac{\partial k_j}{\partial p_j} p_j \right) u_j \quad (12)$$

where u_j is the correction factor and $\sum_{j=1}^{nu} \left(\frac{\partial k_j}{\partial p_j} p_j \right)$ is the sensitivity of the stiffness matrix (S) with respect to the updating parameter:

$$S \cdot u = k_A \frac{Q_A - Q_X}{Q_X} \quad (13)$$

In matrix term the Eq. (13) is written as:

$$[S]_{N \times N} \{u\}_{N \times 1} = [k_A]_{N \times N} \left\{ \frac{Q_A - Q_X}{Q_X} \right\}_{N \times 1}, \quad (14)$$

where *N* is the total degrees of freedom of the structure. The updating correction vector {*u*}, which consists of correction factor of stiffness parameters to update stiffness matrix of the structure. This process is repeated in an iterative way. The performance is judged on the basis of the accuracy with which the deflection predicted by updated FE model match the experimental values.

RESULTS

The results of optimization both of the models in contrast with the experimental measurement are plotted in the Figure 9, description follows.

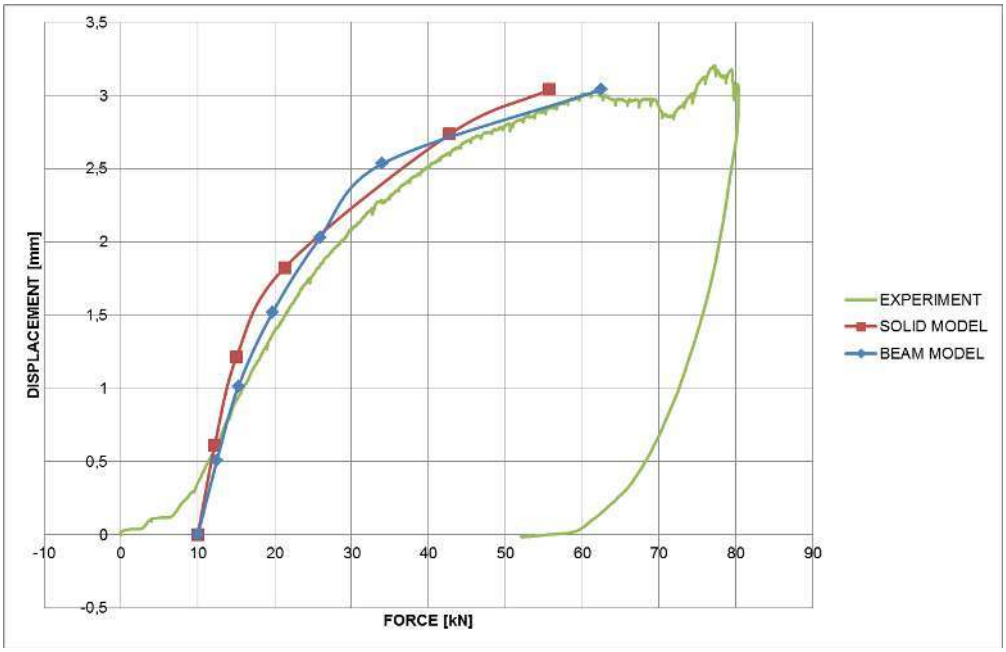

Figure 9 Force – Displacement curve and the deform shape of optimized models

The Beam model optimization

In the ANSYS workbench the Goal Driven Optimization has been done. The input parameters were both longitudinal and torsional stiffness as well as a yield stress of the non-linear materials. In the very beginning stage of the optimization was seen that the most affecting parameters are longitudinal stiffness. Unfortunately the final total deformed shape of the FE model did not correspond with the deformed shape of the real anchor. Because of that, the input parameters of longitudinal stiffness were abandoned and left with the initial values and all optimization was focused only on the torsional stiffness and material properties. The values of the final optimized Beam model and the Initial beam model are shown in Table 2. Figure 10 demonstrates the final deformation. It can be observed from the Figure 9, that the force – displacement curve predicted by the FE model matches well with the experimental curve

Table 2 - The input values of the Initial beam model and optimized values of the Beam model

INITIAL BEAM MODEL					BEAM MODEL
STIFNESS	NAMED			MN/m	MN/m
LONGITUNIDAL	R	Y		406,90	406,90
LONGITUNIDAL	L	Y		406,90	406,90
LONGITUNIDAL	L	X		1470,00	1470,00
LONGITUNIDAL	R	X		1470,00	1470,00
				MNm/rad	MNm/rad
TORSIONAL	L			0,10	2,41
TORSIONAL	R			0,10	2,41
				MN/m	MN/m
LONGITUNIDAL	RN	D	Y	21630,00	21630,00
LONGITUNIDAL	RN	D	X	387,90	387,90
LONGITUNIDAL	RN	U	Y	21630,00	21630,00
LONGITUNIDAL	RN	U	X	387,90	387,90
				MNm/rad	MNm/rad
TORSIONAL	RN	D		0,10	0,11
TORSIONAL	RN	U		0,10	0,11
				MN/m	MN/m
LONGITUNIDAL	UL	X		0,10	0,10
				MN/m	MN/m
LONGITUNIDAL	LN	D	Y	9000,00	9000,00
LONGITUNIDAL	LN	D	X	351,90	351,90
LONGITUNIDAL	LN	U	Y	9000,00	9000,00
LONGITUNIDAL	LN	U	X	351,90	351,90
				MNm/rad	MNm/rad
TORSIONAL	LN	D		0,01	0,34
TORSIONAL	LN	U		0,01	0,34
MATERIAL				MPa	MPa
STRUCTURAL STEEL NL S235				200	200
STRUCTURAL STEEL NL 4.8				300	275
STRUCTURAL STEEL NL 8.8				580	550

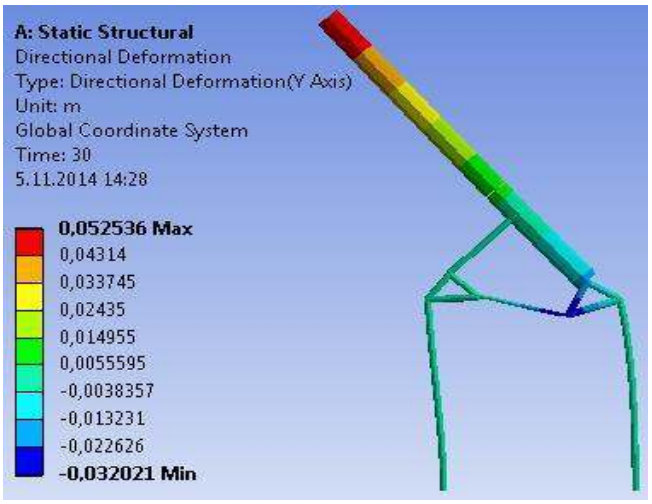

Figure 2 - The deformed shape of the beam model

The Solid model optimization

Since contacts between all parts were modeled as joints, material properties represent the only possible input parameters. The Goal Driven Optimization has been carried out in the ANSYS workbench again. Optimized values are shown in the Table 3 and a final deformed shape is on the Figure 11. It can also be observed from the Figure 9 that the FE predicted force – displacement curve matches well with the experimental curve.

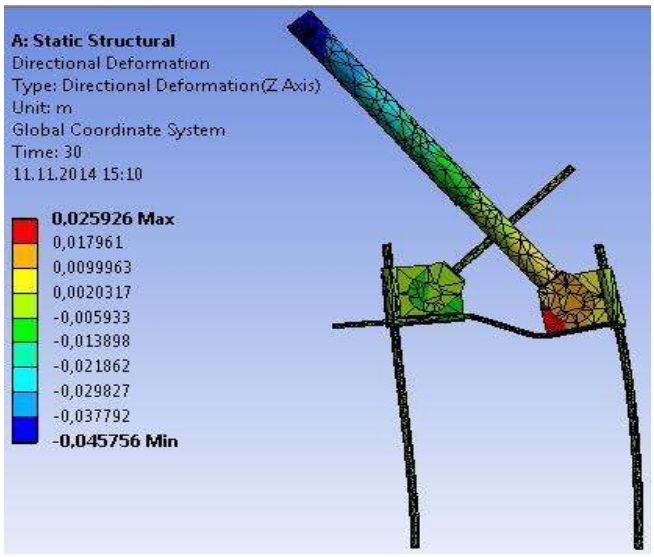

Figure 3 - The deform shape of the solid model

Table 3 - The input values of the Initial solid model and optimized values of the Solid model

INITIAL SOLID MODEL		SOLID MODEL
	MPa	MPa
STRUCTURAL STEEL NL S235	200	200
STRUCTURAL STEEL NL 4.8	300	260
STRUCTURAL STEEL NL 8.8	580	500

CONCLUSIONS

In this paper the new type III (The Oblique Sliding Scaffold Anchor) has been developed and experiments have been conducted to evaluate the behavior of the anchor. The finite elements models (both beam and solid model) were developed. It has been observed, that the finite element models do not match with the experimental results. A choice of updating parameters on the basis of engineering judgment considering the possible locations of modelling errors in a structure is one of the strategies to ensure that only physical meaningful corrections are made. In case of an anchor, modelling of stiffness of the joints and values of the materials are expected to be dominant sources of inaccuracy in the FE model, assuming that the geometric parameters are correctly known. After updating joint stiffness of the joints of the anchor, the finite element prediction matches with experimental results.
This paper is a part of the long term developing of a new fixing system for the façade scaffolding. Based on the FE models developed in this paper the anchor will be optimized to carry support forces adjusted in the new fixing system.

Acknowledgements

The authors are grateful to the financial supports by the Czech Technical University (Project no. SGS17/124/OHK1/2T/11) and also to the program ERASMUS+ (CZ PRAHA10). The technical support and a supervision during experiments by Jonáš of HILTI is gratefully acknowledged as well as support from Experimental Centre of Faculty of the Civil Engineering, CTU in Prague, and Mr. Picek, PKL servis.

REFERENCES

Ansys Workbench, version 14.0.0 – Static Structural
Arora V., Singh S.P., Kundra T.K. (2009). „Damped FE model updating using complex updating parameters: its use for dynamic design.” *Journal of Sound and Vibration*, 324(1-2), 350-364.
Arora V., Singh S.P., Kundra T.K. (2009). “Finite element model updating with damping identification.” *Journal of Sound and Vibration*, 324(3-5), 1111-1123.

Arora V. (2014). “Constrained antiresonance frequencies based model updating method for better matching of FRFs.” *Inverse problems in Science and Engineering*, 22(6), 873-888.
Beale, R.G., Godley, M.H.R. (2009). “Numerical modeling of full-scale tube and fitting scaffold tests,” *Proc. 7th Euromech solid mechanics conference*; Instituto Superior Técnico, Lisbon, Portugal.
Beale, R.G. (2014). “Scaffold research – A review.” *Journal of Constructional Steel Research*, 98, pp. 188-200
CEN (2003). *EN 12811-1: Temporary works equipment – Part 1: Scaffolds – Performance requirements and general design*. European Committee for Standardization
Chandrangsu, T. and Rasmussen, K.J.R. (2009). ”Geometric imperfection measurements and joint stiffness of support scaffold systems.” Proc. 6th *International Conference on Advances Steel Structures*, Vol. 1, University of Lisbon, Portugal, pp. 1075-82.
Chandrangsu, T. and Rasmussen, K. (2011). ”Investigation of geometric imperfections and joint stiffness of support scaffold systems.” *Journal of Constructional Steel Research*, NSW, 67(4), pp. 576-84.
Chandrangsu, T., Rasmussen, K. (2011). “Structural modelling of support scaffold systems.” *Journal of Constructional Steel Research*, 67(5), 866-875.
Dolejš, J., Picek, Z., Škréta, K., Vlasák, M., Vlasák, S. (2011). ” *Navrhování konstrukcí z lešení I*.” Česká technika, CTU in Prague, pp. 28-35. *(Czech text)*
Dolejš, J. (2013). “Spatial coaction of facade scaffolds elements and components.” *Habilitation thesis*, CTU in Prague, Prague, CZ. *(Czech text)*
Enerpac technical data sheet. (02/2010), from http://www.enerpac.com/sites/default/files/e326e_8208_gb_0.pdf
Gant F., Rouch Ph., Louf F., Champaney L. (2011). “Definition and updating of simplified models of joint stiffness.” *International Journal of Solids and Structures,* 48(5), 775-784.
Ilčík, J. and Dolejš, J. (2013). “The Oblique Sliding Scaffold Anchor.” *Utility model* CZ26024, Prague, CZ.
Ilčík, J. and Dolejš, J. (2013). “The Oblique Scaffold Anchor.” *Utility model* CZ26023, Prague, CZ.
Ilčík, J., Dolejš, J. (2013). “The Rigid Scaffold Anchor.” *Utility model* CZ26022, Prague, CZ.
Liu, H., Zhao, Q., Wang, X., Zhou, T., Wang, D., Liu, J. and Chen, Z. (2010). “Experimental and analytical studies on the stability of structural steel tube and coupler scaffolds without X-bracing.” *Engineering Structures*, 32(4), pp. 1003-1015.
Okasha N.M., Frangopol D.M. and Orcesi A.D. (2012). “Automated finite element updating using strain data for the lifetime reliability assessment of bridges.” *Reliability Engineering and System Safety*, 99, pp. 139-150.
Peng, J., Chen, K., Chan, S., Chen, W. (2009). “Experimental and analytical studies on steel scaffolds under eccentric loads.” *Journal of Constructional Steel Research*; 65(2), pp. 422-435.
Peng, J., Wu, Ch., Chan, S., Huang, Ch. (2013). “Experimental and numerical studies of practical systems scaffolds.” *Journal of Constructional Steel Research* 91, pp. 64-75.
Prabhakaran, U., Beale, R. and Godley, M. (2011). “Analysis of scaffolds with connections containing looseness.” *Computers and Structures*, 89(21-22), pp. 1944-55.
Vlasák, S. (2011). *Konstrukce z lešení podle evropských norem*; CTU in Prague, Faculty of Civil Engineering, Prague, CZ, pp. 128-30. *(Czech text)*
Tensiometric dynamometer S-35 data sheet. (02/2011), from http://www.lukas-tenzo.cz/?i=219/tenzometricky-silomer-s-35-s-35-a
Wang, F., Tamura, Y. and Yoshida, A. (2013). ”Wind loads on clad scaffolding with different geometries and building opening ratios.” *Journal of Wind Engineering and Industrial Aerodynamics*, 120(37), pp. 37-50.
Wang, F., Tamura, Y., Yoshida, A. (2014). ”Interference effect of a neighboring building on wind loads on scaffolding.” *Journal of Wind Engineering and Industrial Aerodynamics*,125, pp. 1-12.